Tuning Haptotropic Rearrangements of Arene–Chromium Complexes: Steric and Electronic Effects of Phosphorus Coligands**

Holger Christian Jahr,[a] Martin Nieger,[b] and Karl Heinz Dötz*[a]

Abstract: (η^6-Arene)tricarbonylchromium **2** was synthesised by [3+2+1] benzannulation of the Fischer carbene complex **1** and converted to the thermodynamically more favorable regioisomer **3** by haptotropic metal migration. Photo-induced ligand-exchange reactions in both regioisomers with triphenylphosphine, triphenylphosphite, trimethylphosphine, and trimethylphosphite afforded dicarbonyl(phosphine or phosphite)arene complexes **4**–**11**. The regioisomers were separated by high-performance liquid chromatography (HPLC), and kinetic analyses of the thermo-induced haptotropic metal shift were performed with regioisomers **4**, **6**, **8**, and **10**. The kinetic parameters were compared with those obtained for the parent tricarbonyl complex **2** and were discussed in terms of the steric and electronic properties of the phosphorus ligands by applying a quantitative analysis of ligand effects (QALE). The molecular structures of regioisomeric PPh_3 and $P(OPh)_3$ complexes **4**/**5** and **6**/**7** as well as of $P(OMe)_3$ complex **10** have been established by single-crystal X-ray analysis.

Keywords: arene complexes · chromium · haptotropic metal migration · ligand effects · molecular switches · phosphorus ligands

Introduction

The phenomenon of the haptotropic metal migration occurs with π complexes of transition metals in which the π-bound ligand features multiple coordination possibilities.[1] It has been reported for various metals and a wide array of—cyclic or acyclic—π ligands including sandwich and half-sandwich complexes. Examples for sandwich complexes include haptotropic shifts of cyclopentadienylrhodium(II) or cyclopentadienyliridium(II) moieties,[2] while tricarbonyl(η^6-arene)chromium complexes represent the most extensively studied half-sandwich compounds.[1a,f–i,3] The regioisomers involved in haptotropic migration differ in the mode and site of coordination of a fused arene to the tricarbonylchromium fragment. Most reports deal with haptotropic migrations across naphthalene derivatives, but metal shifts in more extended aromatic π systems are also known.[4] If the regioisomers differ significantly in their thermodynamic stabilities, the rearrangement may be regarded as (thermally) irreversible; in contrast, comparable stabilities of regioisomers result in a dynamic equilibrium.[1f–h,3a,3b] The mechanism of the rearrangement has been established for different conditions; in principle, either an intramolecular, a bimolecular, or a dissociative mechanism may account for the isomerisation. Studies involving enantiopure complexes indicated that in non-coordinative solvents these reactions strictly proceed in an intramolecular manner, implying that the chromium moiety is shifted along the same face of the arene ligand.[5] In general, the haptotropic rearrangement has been studied for complexes that represent the kinetic reaction products (which may be formed in low-temperature complexation or chromium-templated [3+2+1] benzannulation[6]) which subsequently undergo a thermo-induced metal shift. We recently demonstrated that haptotropic rearrangements may also occur against the thermodynamically favoured direction as a result of a proper adjustment of the coligand sphere after photochemical induction.[5b] This strategy allowed control of the coordination site in arene chromium complexes. We now report on how the reaction rate of thermo-induced metal migrations may be tuned by phosphorus coligands differing in their stereoelectronic properties.

[a] Dr. H. C. Jahr, Prof. Dr. K. H. Dötz
Kekulé-Institut für Organische Chemie und Biochemie
Rheinische Friedrich-Wilhelms-Universität Bonn
Gerhard-Domagk-Strasse 1, 53121 Bonn (Germany)
Fax: (+49) 228-73-5813
E-mail: doetz@uni-bonn.de

[b] Dr. M. Nieger
Institut für Anorganische Chemie
Rheinische Friedrich-Wilhelms-Universität Bonn
Gerhard-Domagk-Strasse 1, 53121 Bonn (Germany)

[**] Reactions of complex ligands, Part 100; Part 99: N. D. Hahn, M. Nieger, K. H. Dötz, *J. Organomet. Chem.* **2004**, *689*, 2662–2673.

 DOI: 10.1002/chem.200400674

Results and Discussion

Ligand-exchange reactions of tricarbonyl(naphthalene)chromium complexes: The tricarbonylchromium complex **2** was synthesised by the regioselective chromium-templated [3+2+1] benzannulation of the Fischer carbene complex **1** and 3-hexyne at 55 °C followed by silylation with *tert*-butyldimethylsilyl chloride in the presence of triethylamine to increase its stability towards oxidation (Scheme 1).[6] The regioisomer

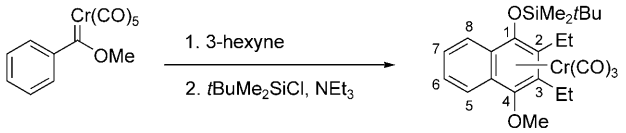

1 **2**

Scheme 1. Regioselective preparation of tricarbonyl(arene)chromium complexes by [3+2+1] benzannulation.

2 represents the product of kinetic reaction control; it may be transformed into its thermodynamically favoured isomer **3** by heating a solution of **2** in di-*n*-butyl ether. With respect to the lability of tricarbonyl(naphthalene)chromium, the synthesised complexes are remarkably inert against an exchange of the arene ligand, which is attributed to the substitution pattern of the arene ligand: It was observed that alkoxy and siloxy substituents stabilise the arene–metal bond.[7]

For the synthesis of the phosphine- and phosphite-substituted chromium complexes **4**–**11**, both complex **2** and its regioisomer **3** were photo-decarbonylated, and the coordinatively unsaturated intermediate was stabilised by adding an excess of cyclooctene prior to photolysis.[8] Initially, **2** was used as the starting material; the dicarbonylchromium complexes of triphenylphosphine (**4**, **5**), triphenylphosphite (**6**, **7**), trimethylphosphine (**8**, **9**) and trimethylphosphite (**10**, **11**) were obtained in good chemical yields by exchange of the cyclooctene for the phosphorus ligand at room temperature in the dark (Scheme 2). In some cases, the tricarbonyl complex **2** was partially recovered. Surprisingly, the resulting complexes were generally isolated as a mixture of both regioisomers—even if the ligand-exchange reaction was performed with pure regioisomer **2** and at temperatures ranging from −50 °C during irradiation to room temperature for the addition of the phosphine or phosphite. The appearance of the thermodynamically favoured complex isomers was not expected, since free activation enthalpies for haptotropic shifts of $Cr(CO)_3$ units across naphthalene derivatives usually range from about 100 to 130 kJ mol^{-1} and, consequently, a metal migration should not occur at a noticeable rate at room temperature or below.[1i,3] Only very few examples of haptotropic rearrangements in chromium complexes have been reported under similar mild conditions.[9]

The ratio of regioisomeric pairs may vary within a certain range. An average ratio amounts to 2:1 and 3:1 for pairs of

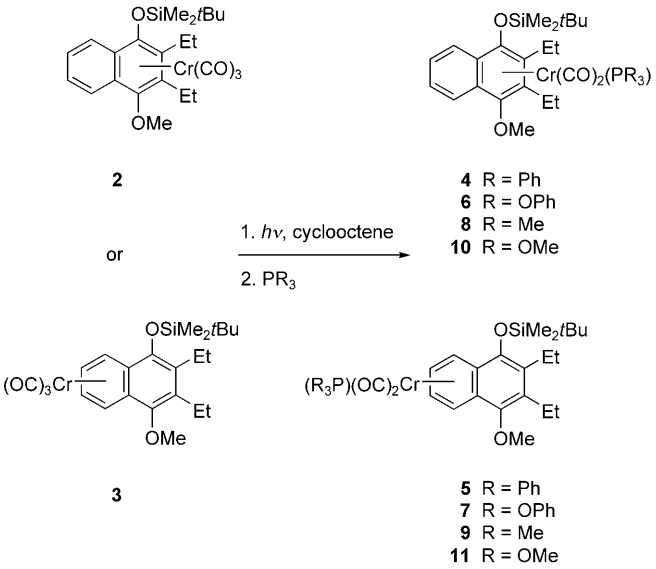

Scheme 2. Synthesis of dicarbonyl(PR_3)chromium complexes by photochemical ligand substitution.

complexes **4**/**5** and **6**/**7**, respectively, whereas a 6:1 ratio is observed for complexes **8**/**9** and **10**/**11** indicating that PMe_3 and $P(OMe)_3$ complexes **8** and **10** are less susceptible to a metal shift than their PPh_3 and $P(OPh)_3$ congeners **4** and **6**.

We recently reported on how a haptotropic metal shift may occur against the thermodynamically favoured direction (Scheme 3).[5b] Under thermal conditions, complex **2** reacts

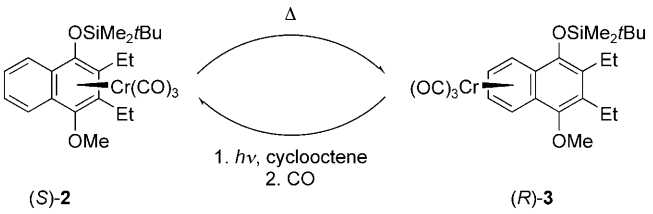

Scheme 3. Thermo-optical switch based on a haptotropic metal shift.

irreversibly to its regioisomer **3**; a properly adjusted coligand sphere of the chromium template, however, allows a reconversion of **3** into **2**. In this respect, two consecutive ligand-exchange reactions lead from the thermodynamically more stable isomer **3** to the less stable haptotropomer **2** via a cyclooctene complex intermediate, which was subjected to a recarbonylation. We modified the synthetic sequence by adding PPh_3 to the cyclooctene chromium complex instead of CO. As expected, the reaction did not provide pure isomer **5**; instead, it resulted again in a mixture of regioisomers **4** and **5**. The appearance of complex **4** highlights again how haptotropic metal migrations may occur against the favoured direction; the formation of **5** may be obvious at first sight, but in this particular case the ligand exchange is accompanied by two haptotropic metal shifts, one occurring during photolysis, and the second taking place during the substitution of cyclooctene for the phosphine.

For the independent characterisation of each of the eight PR_3 complexes, the regioisomers obtained by ligand exchange were separated by preparative high-performance liquid chromatography. Table 1 provides the relevant ν(CO) absorptions and ^{13}C and ^{31}P chemical shifts observed for the coligand sphere. The molecular structures of the pure haptotropomers **4–7** and **10** were established by X-ray crystallography.

Table 1. Selected IR and NMR data for arene chromium complexes **2–11**.

$Cr(CO)_2(L)$	ν_{CO} A_1 [cm^{-1}][a]	ν_{CO} E/B_1 [cm^{-1}][a,b]	$\delta(^{13}C_{CO})$[c]	$\delta(^{31}P)$[c]
2 L = CO	1961	1896, 1882	233.8	–
3 L = CO	1971	1915, 1907, 1896	232.5	–
4 L = PPh_3	1888, 1882	1844, 1830	242.6, 241.2	86.7
5 L = PPh_3	1900	1853, 1844	240.4, 240.0	90.6
6 L = $P(OPh)_3$	1902	1851, 1844	238.6, 236.9	189.0
7 L = $P(OPh)_3$	1930, 1922	1884, 1875, 1869	234.9, 234.9	201.2
8 L = PMe_3	1888, 1878	1838, 1826	240.5, 239.0	35.0
9 L = PMe_3	1898, 1892	1844, 1836	–	33.4
10 L = $P(OMe)_3$	1898, 1886	1846, 1836	239.1, 237.7	213.3
11 L = $P(OMe)_3$	1909, 1900	1853	237.4, 237.0	214.7

[a] Recorded in petroleum ether. [b] E for **2** and **3**; B_1 for **4–11**. [c] Recorded in $CDCl_3$ (**2–7**, **10** and **11**) or CD_2Cl_2 (**8** and **9**).

Molecular structures of [(arene)Cr(CO)$_2$(PR$_3$)] complexes: For the crystal structure analysis of the phosphorus-substituted chromium complexes, suitable single crystals were grown by slow evaporation of the solvent. For the regioisomers **4** (Figure 1, red crystals) and **5** (Figure 2, black crystals) a diethyl ether solution was used, while red crystals of the $P(OPh)_3$ complexes were obtained from a solution in heptane (**6**, Figure 3) or a mixture of heptane and diethyl

Figure 1. Molecular structure of PPh_3 complex **4**. Color code: Cr: green; P: blue; O red, Si: violet; C: black. Hydrogen atoms have been omitted for clarity. Selected bond lengths [Å]: Cr1–P1 2.3123(12), Cr1–C1 2.232(4), Cr1–C2 2.208(5), Cr1–C3 2.219(5), Cr1–C4 2.264(4), Cr1–C4a 2.317(4), Cr1–C8a 2.291(4), C1–C2 1.395(7), C2–C3 1.458(7), C3–C4 1.401(6), C4–C4a 1.435(6), C4a–C8a 1.438(6), C8a–C1 1.443(6); selected torsion angles [°]: C5-C4a-C8a-C1 176.3(4), C4-C4a-C8a-C8 178.0(4), Cr1-P1-C1p-C2p −172.7(3), Cr1-P1-C7p-C8p −65.6(3), Cr1-P1-C13p-C14p 141.5(3).

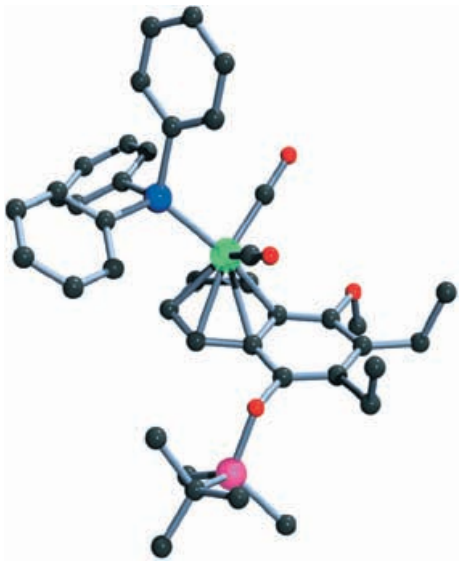

Figure 2. Molecular structure of PPh_3 complex **5**. Color code: Cr: green; P: blue; O red, Si: violet; C: black. Hydrogen atoms have been omitted for clarity. Selected bond lengths [Å]: Cr1–P1 2.2947(17), Cr1–C4a 2.271(5), Cr1–C5 2.195(5), Cr1–C6 2.204(5), Cr1–C7 2.200(5), Cr1–C8 2.210(5), Cr1–C8a 2.266(5), Cr1–Z_{Ar} 1.711(5), C1–C2 1.382(7), C2–C3 1.417(8), C3–C4 1.417(8), C4–C4a 1.394(7), C4a–C8a 1.423(7), C8a–C1 1.428(7); selected torsion angles [°]: C5-C4a-C8a-C1 −176.4(4), C4-C4a-C8a-C8 178.1(4), Cr1-P1-C1p-C2p 102.9(5), Cr1-P1-C7p-C8p −37.1(5), Cr1-P1-C13p-C14p −168.6(3).

Figure 3. Molecular structure of $P(OPh)_3$ complex **6**. Color code: Cr: green; P: blue; O red, Si: violet; C: black. Hydrogen atoms have been omitted for clarity. Selected bond lengths [Å]: Cr1–P1 2.1993(7)/2.2047(7), Cr1–C1 2.259(2)/2.279(2), Cr1–C2 2.213(2)/2.217(2), Cr1–C3 2.244(2)/2.2320(19), Cr1–C4 2.229(2)/2.222(2), Cr1–C4a 2.297(2)/2.281(2), Cr1–C8a 2.354(2)/2.333(2), Cr1–Z_{Ar} 1.761(1)/1.755(1), C1–C2 1.412(3)/1.407(3), C2–C3 1.439(3)/1.443(3), C3–C4 1.405(3)/1.402(3), C4–C4a 1.430(3)/1.428(3), C4a–C8a 1.431(3)/1.429(3), C8a–C1 1.431(3)/1.433(3); selected torsion angles [°]: C5-C4a-C8a-C1 −176.95(19)/177.02(18), C4-C4a-C8a-C8 −171.62(19)/175.56(18), P1-O1p-C1p-C2p 99.3(2)/50.9(3), P1-O2p-C7p-C8p 118.9(2)/-69.2(2), P1-O3p-C13p-C14p −112.7(2)/132.01(17).

ether (**7**, Figure 4), respectively. The $P(OMe)_3$ complex **10** (Figure 5) provided dark red crystals from a toluene solution.

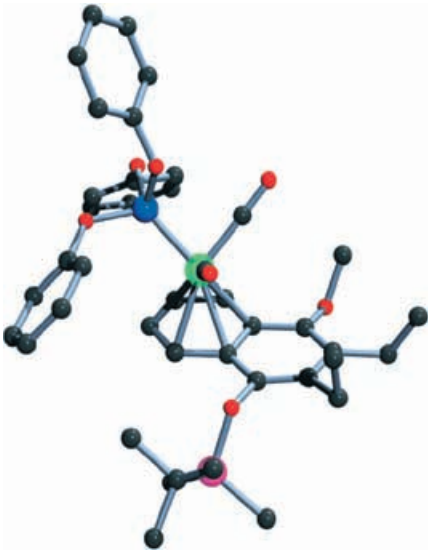

Figure 4. Molecular structure of $P(OPh)_3$ complex **7**. Color code: Cr: green; P: blue; O red, Si: violet; C: black. Hydrogen atoms have been omitted for clarity. Selected bond lengths [Å]: Cr1–P1 2.1771(6), Cr1–C4a 2.278(2), Cr1–C5 2.212(2), Cr1–C6 2.2304(19), Cr1–C7 2.2192(19), Cr1–C8 2.207(2), Cr1–C8a 2.273(2), Cr1–Z_{Ar} 1.734(1), C1–C2 1.372(3), C2–C3 1.441(3), C3–C4 1.367(3), C4–C4a 1.439(3), C4a–C8a 1.428(3), C8a–C1 1.428(3); selected torsion angles [°]: C5-C4a-C8a-C1 −176.45(17), C4-C4a-C8a-C8 179.22(17), P1-O1p-C1p-C2p −130.61(16), P1-O2p-C7p-C8p 108.2(2), P1-O3p-C13p-C14p 84.2(2).

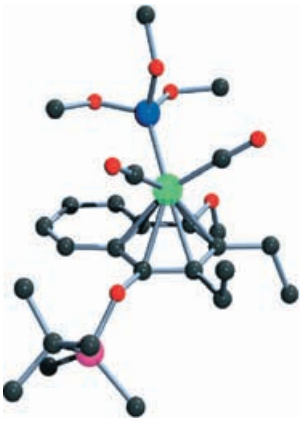

Figure 5. Molecular structure of $P(OMe)_3$ complex **10**. Color code: Cr: green; P: blue; O red, Si: violet; C: black. Hydrogen atoms have been omitted for clarity. Selected bond lengths [Å]: Cr1–P1 2.2274(6), Cr1–C1 2.2285(19), Cr1–C2 2.2216(18), Cr1–C3 2.2211(18), Cr1–C4 2.2263(19), Cr1–C4a 2.2739(18), Cr1–C8a 2.2759(18), Cr1–Z_{Ar} 1.728(1), C1–C2 1.413(3), C2–C3 1.430(3), C3–C4 1.414(3), C4–C4a 1.432(3), C4a–C8a 1.431(3), C8a–C1 1.447(3); selected torsion angles [°]: C5-C4a-C8a-C1 179.08(16), C4-C4a-C8a-C8 177.31(16), Cr1-P1-O1p-C1p −57.52(14), Cr1-P1-O2p-C2p 57.87(15), Cr1-P1-O3p-C3p 179.73(15).

The crystal structure of PPh_3 complex **4** (Figure 1) reveals a conformation with a distorted organometallic unit; whereas the Cr–P bond is staggered relative to the carbon atoms C4 and C4a, one carbonyl ligand is eclipsed with respect to C1. A similar distortion is observed in the crystal structure of the $P(OPh)_3$ complex **6**. This crystal contains both enantiomers of **6**, but each in a different crystallographic position, which implies the chirality of the crystal itself. In both positions the Cr–P bond is eclipsed with respect to the carbon atom C4 and one carbonyl ligand is staggered between the C2 and C3. The haptotropically rearranged isomer **7** displays a staggered conformation of the organometallic unit (Figure 4): The Cr–P bond is situated between the carbon atoms C6 and C7. An eclipsed conformation is observed for the haptotropically rearranged complex **5** (Cr–P and C7, CO ligands and C5/C8a) as well as for the $P(OMe)_3$ complex **10** (Cr–P and C4a, CO ligands and C1/C3). The lengths measured for the Cr–P bonds are remarkably short when compared to those in analogous $Cr(PR_3)$ complexes (**4**: 2.31, **5**: 2.29, **6**: 2.20/2.20, **7**: 2.18, **10**: 2.23 Å).

Similar to the situation in the crystal structures of the tricarbonyl complexes **2** and **3**,[5b] the chromium atom is bonded to the coordinated aromatic ring in a non-concentric way in the $[Cr(CO)_2(PR_3)]$ complexes **4**–**7** and **10**. The conformation of the triphenylphosphine complex with the phosphorus ligand pointing inwards relative to the naphthalene ligand results in long bonds between chromium and the quaternary carbon atoms and short bonds to the ethyl-substituted carbon atoms. A disorder is observed for the *tert*-butyldimethylsilyl group; for the ease of representation only one conformer is depicted in Figure 1. Less deviation from a concentric chromium–arene bond is present in the structural isomer **5**: The bulky PPh_3 ligand points to the exterior of the aromatic system, which decreases the internal strain. In the crystal structure of the triphenylphosphite complex **6**, the chromium atom is shifted to the periphery of the aromatic skeleton as well, but the *syn* position of the silyl protective group leads to a particularly short bond to the methoxysubstituted carbon atom. Again, a smaller degree of deviation from a concentric bond between the chromium atom and the aromatic ring is observed for the coordinative isomer **7**, for which the position of the chromium atom is not influenced by the silyl protective group owing to its *anti* conformation. In the molecular structure of the trimethylphosphite complex **10**, the chromium–arene bond is less unsymmetrical than for the phenyl-substituted phosphorus ligands, which is a result of the *anti* position of the silyl group as well as the low steric demand of the $P(OMe)_3$ ligand.

Alternating bond lengths are observed along the naphthalene system for all complexes, the differences are particularly evident for the $P(OPh)_3$ complex **7**, where short bonds connect the atoms C5–C6 and C7–C8, but also C1–C2 and C3–C4 in the coordinated ring. Details concerning the acquisition and refinement of the crystallographic data are presented in Table 2 and Table 3.

Tuning haptotropic rearrangements of arene–chromium complexes: Half-sandwich $Cr(CO)_3$ complexes of fused arenes are capable of a haptotropic metal shift along the π-ligand system. These rearrangements are most commonly induced by thermal induction, by which the thermodynamical-

Table 2. Collection and refinement data of the structure analyses of complexes **4**, **5** and **6**.

	4	**5**	**6**
empirical formula	$C_{41}H_{47}CrO_4PSi$	$C_{41}H_{47}CrO_4PSi$	$C_{41}H_{47}CrO_7PSi$
M [g mol^{-1}]	714.85	714.85	762.85
T [K]	123(2)	123(2)	123(2)
λ [Å]	0.71073 ($Mo_{K\alpha}$)	0.71073 ($Mo_{K\alpha}$)	0.71073 ($Mo_{K\alpha}$)
crystal system	monoclinic	monoclinic	monoclinic
space group	$P2_1$ (no. 4)	$P2_1/n$ (no. 14)	$P2_1$ (no. 4)
a [Å]	8.8483(2)	9.2357(4)	9.3098(1)
b [Å]	25.2693(7)	12.7247(7)	17.7945(2)
c [Å]	9.2269(3)	32.092(2)	23.2479(3)
α [°]	90	90	90
β [°]	114.895(1)	93.146(2)	95.597(1)
γ [°]	90	90	90
V [Å^3]	1871.35(9)	3765.8(4)	3832.96(8)
Z	2	4	4
crystal dimensions [mm]	0.50×0.30×0.10	0.15×0.08×0.02	0.40×0.30×0.20
ρ_{calcd} = [g cm^{-3}]	1.269	1.261	1.322
μ [mm^{-1}]	0.420	0.418	0.420
F(000)	756	1512	1608
index ranges	$-10 \le h \le 10$	$-10 \le h \le 6$	$-12 \le h \le 11$
	$-30 \le k \le 30$	$-15 \le k \le 14$	$-23 \le k \le 23$
	$-10 \le l \le 10$	$-37 \le l \le 34$	$-29 \le l \le 30$
θ limits	$2.68 \le \theta \le 25.03$	$3.06 \le \theta \le 25.03$	$2.88 \le \theta \le 27.48$
total reflections	20483	10451	41155
unique reflections	6541	5773	17008
parameters	421	433	919
restraints	291	0	1
R for $I > 2\sigma(I)$	0.0476	0.0605	0.0335
wR^2 for all data	0.1299	0.1306	0.0609
Flack's parameter	0.59(2), racemic twin	–	−0.01(1)
goodness-of-fit on F^2	1.021	0.877	0.929

Table 3. Collection and refinement data of molecular structures of complexes **7** and **10**.

	7	**10**
empirical formula	$C_{41}H_{47}CrO_7PSi$	$C_{26}H_{41}CrO_7PSi$
M [g mol^{-1}]	762.85	576.65
T [K]	123(2)	123(2)
λ [Å]	0.71073 ($Mo_{K\alpha}$)	0.71073 ($Mo_{K\alpha}$)
crystal system	monoclinic	triclinic
space group	$P2_1/n$ (no. 14)	$P\bar{1}$ (no. 2)
a [Å]	14.2439(2)	10.2449(2)
b [Å]	13.7903(2)	10.6204(2)
c [Å]	21.1209(3)	13.4430(3)
α [°]	90	91.544(1)
β [°]	109.068(1)	93.510(1)
γ [°]	90	97.488(1)
V [Å^3]	3921.09(10)	1446.57(5)
Z	4	2
crystal dimensions [mm]	0.35×0.15×0.10	0.40×0.25×0.15
ρ_{calcd} = [g cm^{-3}]	1.292	1.324
μ [mm^{-1}]	0.411	0.533
F(000)	1608	612
index ranges	$-16 \le h \le 16$	$-12 \le h \le 12$
	$-16 \le k \le 16$	$-12 \le k \le 12$
	$-25 \le l \le 25$	$-15 \le l \le 15$
θ limits	$2.94 \le \theta \le 25.01$	$2.44 \le \theta \le 25.01$
total reflections	50258	17901
unique reflections	6898	5091
parameters	460	325
restraints	0	0
R for $I > 2\sigma(I)$	0.0338	0.0305
wR^2 for all data	0.0815	0.0845
goodness-of-fit on F^2	0.951	1.055

ly less stable regioisomer is transformed into the more stable one. If the coordination of one aromatic ring is strongly favoured over the other, the haptotropic isomerisation is virtually irreversible; in cases in which both isomers possess comparable thermodynamic stabilities, a dynamic equilibrium is observed. The first example of haptotropic rearrangements involving π ligands derived from naphthalene was reported for $Cr(CO)_3$ complexes of methyl-substituted derivatives.[1a] Subsequent research provided rate constants and thermodynamic activation parameters for π complexes in which the degeneration of the haptotropic rearrangement was removed by selective mono- or polydeuteration,[1f] and the influence of the naphthalene substitution pattern on the kinetics and the thermodynamic equilibrium of the haptotropic interconversion was determined systematically.[3a,b] Haptotropic shifts observed along the addition of phosphines to tricarbonyl complexes of manganese were subjected to molecular orbital calculations; the results of these calculations again emphasised the importance of the substitution pattern present in the polyene.[10] We shall now address the kinetic consequences of a modification of the coligand sphere by photolytic exchange of a carbonyl ligand for a phosphine or phosphite ligand, during which the π-ligand remains unaltered.

To obtain pure samples of the complex regioisomers **4**, **6**, **8** and **10**, the mixtures obtained by ligand exchange were separated by preparative HPLC. Each of these complexes was subjected to a haptotropic rearrangement in hexafluorobenzene at 333 K (**4**, **6** and **10**) or at 348 K (**8** and **10**), which was monitored by ^{1}H NMR spectroscopy (Scheme 4). If distilled and carefully deoxygenated C_6F_6 is used, high quality spectra can be recorded over more than two days and a precise determination of the reaction parameters can be achieved. The results can be compared with those obtained for the parent $Cr(CO)_3$ complex **2** under identical conditions (333 K[5b] and 348 K, hexafluorobenzene). The first-order kinetics of the rearrangement reactions are indicative for intramolecular metal shifts, as is anticipated from previous re-

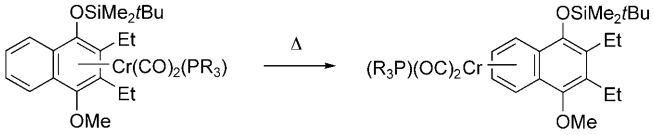

4 R = Ph
6 R = OPh
8 R = Me
10 R = OMe

5 R = Ph
7 R = OPh
9 R = Me
11 R = OMe

Scheme 4. Haptotropic rearrangement of [(arene)$Cr(CO)_2(PR_3)$] complexes.

sults.[1i,3,5] A theoretical study on details of the haptotropic rearrangement is underway and will address the question of the actual pathway of the metal migration.

Two of the phosphorus complexes display an enhanced reactivity: When compared with the metal shift in the parent $Cr(CO)_3$ complex **2**, that for the PPh_3 complex **4** and the $P(OPh)_3$ complex **6** proceeds about 2–3 times faster. A representative molar ratio versus time plot is depicted in Figure 6 for the $P(OPh)_3$ complexes **6**/**7**.

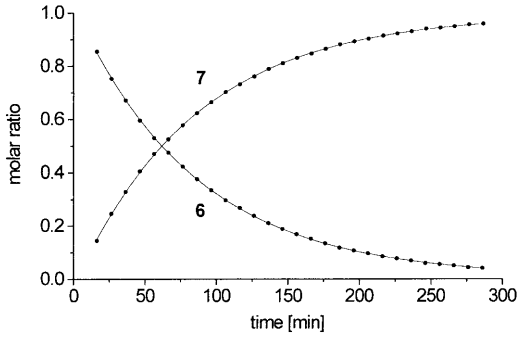

Figure 6. Molar ratio versus time plot for the rearrangement of complex **6** to **7** at 333 K.

On the contrary, the haptotropic migration is hampered when a CO ligand is exchanged for PMe_3 (**8**) or $P(OMe)_3$ (**10**). In comparison to the $Cr(CO)_3$ complex **2**, the $P(OMe)_3$ derivative **10** is an order of magnitude less reactive; the free activation enthalpy for the shift of the $Cr(CO)_2(PMe_3)$ unit is even more increased. To secure sufficiently large rate constants, the haptotropic rearrangement for this complex was studied at an elevated temperature of 348 K (Figure 7).

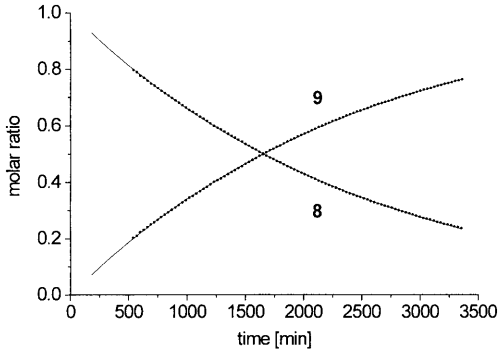

Figure 7. Molar ratio versus time plot for the rearrangement of complex **8** to **9** at 348 K.

To evaluate the results observed for the PMe_3 complex **8**, the haptotropic rearrangements of the tricarbonyl complex **2** and the $P(OMe)_3$ complex **10** were studied at 348 K as well: The PMe_3-substituted complex **8** reacts about 60 times slower than the $Cr(CO)_3$ complex **2**; the resulting free activation enthalpy is the highest observed for a naphthalene bearing the benzannulation pattern. Rate constants and $\Delta G^{\neq}$ values for all haptotropic metal shifts are presented in Table 4; Figure 8 and Figure 9 illustrate a comparison of the rate constants measured at 333 K and 348 K, respectively.

Table 4. Kinetic parameters for the haptotropic rearrangement of $Cr(CO)_2(L)$ complexes **2**, **4**, **6**, **8** and **10**, cone angles θ and electronic parameters χ.

$Cr(CO)_2(L)$	T [K]	k [s^{-1}][a]	$\Delta G^{\neq}$ [kJ mol^{-1}]	θ [°][11]	χ [cm^{-1}][12]
2 L = CO[5b]	333	$(6.5\pm0.7)\times10^{-5}$	108.5 ± 0.3	–	–
2 L = CO	348	$(4.3\pm0.4)\times10^{-4}$	108.1 ± 0.3	–	–
4 L = PPh_3	333	$(1.6\pm0.2)\times10^{-4}$	106.0 ± 0.3	145	13.25
6 L = $P(OPh)_3$	333	$(1.9\pm0.2)\times10^{-4}$	105.6 ± 0.3	128	30.20
8 L = PMe_3	348	$(7.2\pm0.7)\times10^{-6}$	119.9 ± 0.3	118	08.55
10 L = $P(OMe)_3$	333	$(6.1\pm0.6)\times10^{-6}$	115.1 ± 0.3	107	24.10
10 L = $P(OMe)_3$	348	$(3.4\pm0.3)\times10^{-5}$	115.5 ± 0.3	107	24.10

[a] Recorded in C_6F_6.

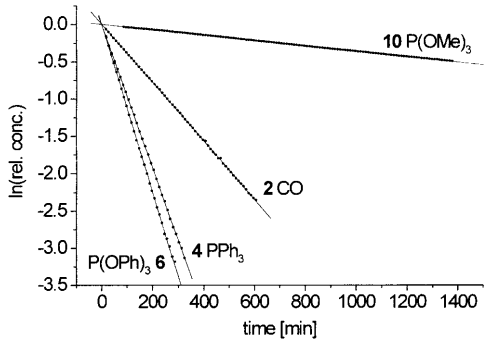

Figure 8. Tuning of rate constants for the haptotropic rearrangement by variation of the coligand sphere (333 K).

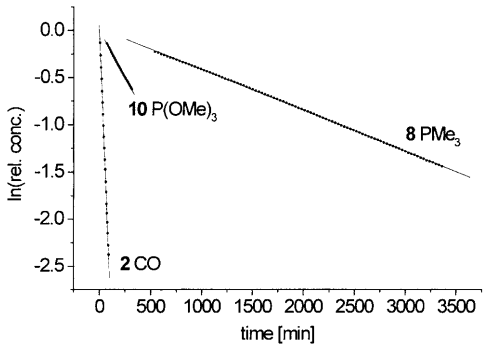

Figure 9. Rate constants for the PMe_3 complex **8**, the $P(OMe)_3$ complex **10** and the parent tricarbonyl complex **2** at 348 K.

Having demonstrated how a haptotropic metal migration may be tuned by modification of the coligand sphere, we aimed at a quantitative analysis of the steric and electronic ligand effects (QALE).[11,13] Since the rate constants were measured at two distinct temperatures and $\Delta G^{\neq}$ values revealed only a slight temperature dependence, we chose the free activation enthalpy as the property to be analysed by this method. To secure a correlation of the kinetic analysis of the PMe_3 complex **8**, which was performed at 348 K, with

studies of the more reactive PPh_3 complex **4** and the $P(OPh)_3$ complex **6**, which were carried out at 333 K, the rearrangements of the $P(OMe)_3$ complex **10** and parent tricarbonyl complex **2** were examined at both temperatures.

The most original approach in quantifying steric and electronic effects of phosphorus ligands was suggested by Tolman who introduced the cone angle θ as a measure of the steric demand and the wavenumber of the A_1 ν(CO) stretching frequency in $[Ni(CO)_3(PR_3)]$ as a measure of the electronic property of the coligand.[11] The latter is sometimes represented as the χ value which reflects the total hypsochromic shift (in cm^{-1}) with respect to the model ligand $PtBu_3$.

$$\Delta G^{\neq} = a\theta + b\chi + c \quad (1)$$

An analysis according to Equation (1) was performed on the basis of Tolman's cone angles θ and accurately determined χ values.[12] This analysis indicates that both steric and electronic properties of the phosphorus ligands contribute significantly to the free activation enthalpy (Figure 10,

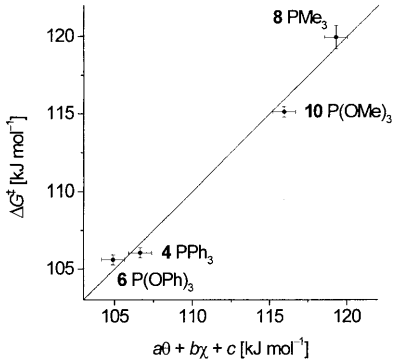

Figure 10. Fit of the experimental $\Delta G^{\neq}$ values versus $a\theta + b\chi + c$.

$a = (-0.383 \pm 0.051)$ kJ mol^{-1} per °, $b = (-0.486 \pm 0.083)$ kJ mol^{-1} cm^{-1}, $c = (168.6 \pm 6.9)$ kJ mol^{-1}, $R^2 = 0.987$ for the set of four PR_3 complexes). Parameter a reflects the influence of the ligands' steric bulk, while parameter b provides a measure for the impact of its electronic characteristics. Neither coefficient may be neglected to rationalise the $\Delta G^{\neq}$ values observed, which implies that the rate constants correlate with both the steric and the electronic properties of the phosphorus ligands. It is evident that the haptotropic shift of the organometallic fragment is enhanced by introducing bulky and/or electron-deficient coligands. On the other hand, the activation barrier increases when CO is substituted for electron-rich phosphines with poor steric demand (such as PMe_3). Even though the fit of the experimental data to Equation (1) is quite satisfactory, it may be further improved by increasing the original Tolman value for the cone angle θ of $P(OMe)_3$ as has been suggested by several groups.[14]

Conclusions

$[Cr(CO)_2(PR_3)]$ complexes of naphthalene derivatives have been synthesised in high yields by photo-induced ligand substitution via cyclooctene intermediates. The ligand exchange is partially accompanied by low-temperature haptotropic metal migration, which affords both possible regioisomers for each phosphorus ligand. An additional metal shift occurs already during photolysis if the thermodynamically more stable $Cr(CO)_3$ complex serves as starting material. Upon thermal induction the thermodynamically less stable PR_3 complex may be converted into its thermodynamically more stable regioisomer: The kinetics of these rearrangements reveal that rate constants for the metal shift can be tuned by a proper choice of phosphine or phosphite coligands. Compared to the parent tricarbonyl complex the PPh_3- and $P(OPh)_3$-substituted derivatives display an enhanced reactivity, whereas the rearrangement is slowed down for the PMe_3 and $P(OMe)_3$ complexes. A QALE analysis of the free activation enthalpy of the process indicates significant contributions from both steric and electronic properties of the PR_3 ligands. $\Delta G^{\neq}$ is increased for small electron-rich phosphines, whereas electron-deficiency or increased steric demand enhances the haptotropic isomerisation.

Experimental Section

General reaction conditions, instrumentation and reagents: All reactions were performed under an argon atmosphere. Solvents used for reactions, crystallisation and chromatography were dried by distillation from lithium aluminium hydride (diethyl ether, petroleum ether), calcium hydride (di-*n*-butyl ether, dichloromethane, hexafluorobenzene) or sodium (toluene). Column chromatography was performed with degassed silica gel (Machery Nagel, type 60, 0.015–0.025 mm). For HPLC, Knauer Eurospher 100 Si and Knauer Euroshper 100 CN columns were used; the flow was adjusted to 1 mL min^{-1} for analytical HPLC. Analyses were performed with a Nicolet Magna 550 FT-IR, with Bruker DRX 500 and DPX 300 NMR spectrometers and a Kratos MS 50 (70 eV) mass spectrometer. The abbreviation "t" is used in the analytical section to denote a pseudo-triplet. Pentacarbonyl[methoxy(phenyl)carbene]chromium (**1**) was synthesised by addition of phenyllithium to chromium hexacarbonyl in *tert*-butyl methyl ether at 0 °C, followed by treatment with trimethyloxonium tetrafluoroborate in dichloromethane at room temperature and purification by column chromatography. Tricarbonyl[(η^6-1,2,3,4,4a,8a)-1-*tert*-butyldimethyl-silyloxy-2,3-diethyl-4-methoxynaphthalene]chromium (**2**) was prepared according reference [3b].

X-ray crystallographic studies of 4, 5, 6, 7 and 10: Crystals for X-ray analysis were grown by slow evaporation of the solvent at room temperature. Solutions of the PPh_3 complexes **4** and **5** in diethyl ether gave red crystals of **4** and black crystals of **5**, respectively. Red crystals of the $P(OPh_3)$ complexes **6** and **7** were grown from heptane (**6**) or a mixture of heptane and diethyl ether (**7**). A toluene solution of the $P(OMe)_3$ complex **10** yielded dark red crystals. Crystallographic data were collected with a Nonius KappaCCD diffractometer at 123 K. The molecular structures were solved by direct methods. Hydrogen atoms were located by using a riding model. Details of the collection and refinement of the data are presented in Table 2. CCDC 278109 (**4**), 278110 (**5**), 278111 (**6**), 278112 (**7**), and 278113 (**10**) contain the supplementary crystallographic data for this paper. These data can be obtained free of charge from The Cambridge Crystallographic Data Centre via www.ccdc.cam.ac.uk/data_request/cif

General procedure for the synthesis of the (arene)Cr(CO)$_2$(PR$_3$) complexes 4–11: A solution of the tricarbonyl complex **2** or **3** and cyclooctene (7.5 mL) in petroleum ether (200 mL) was irradiated by using a medium-pressure mercury lamp (125 W) with a pyrex filter at −50 °C until complete removal of one equivalent CO (IR spectrum of the cyclooctene complex (petroleum ether): $\tilde{\nu}$ = 1907 (vs), 1849 (vs) cm^{-1}). The volume of the solution was reduced to 50 mL in vacuo and the respective phosphine or phosphite was added as a solution in petroleum ether (toluene in the case of PMe_3) and stirred at room temperature until the ligand exchange was complete. After removal of volatile components, the residue was subjected to column chromatography and the fraction containing the dicarbonyl complexes was separated by HPLC.

Synthesis of dicarbonyl(triphenylphosphine)[(η^6-1,2,3,4,4a,8a)-1-*tert*-butyldimethylsilyloxy-2,3-diethyl-4-methoxynaphthalene]chromium (4) and dicarbonyl(triphenylphosphine)[(η^6-4a,5,6,7,8,8a)-1-*tert*-butyldimethylsilyloxy-2,3-diethyl-4-methoxynaphthalene]chromium (5): The reaction was carried out with tricarbonyl complex **3** (0.26 g, 0.55 mmol) and triphenylphosphine (0.15 g, 5.8 mmol). Eluent for column chromatography: dichloromethane/petroleum ether (3/2). Overall yield: 0.37 g (0.52 mmol, 95 %) of a dark red solid. Analytical HPLC: Knauer Eurospher 100 Si, 99 % *n*-hexane, 1 % diethyl ether, retention times: 4.80 min (**4**), 5.78 min (**5**).

Complex **4**: Yield: 0.25 g (0.35 mmol, 64 %) of a dark red solid. R_f (dichloromethane/petroleum ether 3/2) = 0.75; ^{1}H NMR (500 MHz, $CDCl_3$): δ = 7.79 (d, $^3J_{H,H}$ = 8.8 Hz, 1H; H8), 7.28–7.23, 7.17–7.11 (m, 16H; H7/6, 3C$_6$H$_5$), 6.89 (d, $^3J_{H,H}$ = 8.5 Hz, 1H; H5), 6.84 ("t", 1H; H6/7), 3.53 (s, 3H; OCH_3), 2.99 (dq, $^2J_{H,H}$ = 14.6 Hz, $^3J_{H,H}$ = 7.5 Hz, 1H; CH_2), 2.87 (dq, $^2J_{H,H}$ = 14.9 Hz, $^3J_{H,H}$ = 7.5 Hz, 1H; CH_2), 2.79 (dq, $^2J_{H,H}$ = 14.9 Hz, $^3J_{H,H}$ = 7.5 Hz, 1H; CH_2), 2.74 (dq, $^2J_{H,H}$ = 14.6 Hz, $^3J_{H,H}$ = 7.5 Hz, 1H; CH_2), 1.41 (t, $^3J_{H,H}$ = 7.5 Hz, 3H; CH_2CH_3), 1.34 (t, $^3J_{H,H}$ = 7.5 Hz, 3H; CH_2CH_3), 1.12 (s, 9H; $C(CH_3)_3$), 0.49 (s, 3H; $SiCH_3$), 0.38 ppm (s, 3H; $SiCH_3$); ^{13}C NMR (125 MHz, $CDCl_3$): δ = 242.6 (d, $^2J_{P,C}$ = 19.7 Hz; Cr(CO)), 241.2 (d, $^2J_{P,C}$ = 18.7 Hz; Cr(CO)), 137.4 (d, $^1J_{P,C}$ = 32.2 Hz; 3PC), 133.3 (d, $^2J_{P,C}$ = 11.0 Hz; 6PC*C*H), 128.2 (3PCCH*C*H*C*H), 127.1 (d, $^3J_{P,C}$ = 8.6 Hz; 6PCCH*C*H), 126.8 (ArCH), 126.5, 126.4 (C1, C4) 125.6, 125.0, 123.0 (3 ArCH), 104.2, 100.6, 98.3, 97.1 (C2, C3, C4a, C8a), 62.0 (OCH_3), 26.4 ($C(CH_3)_3$), 21.2, 21.2 ($2CH_2$), 19.3 ($C(CH_3)_3$), 15.9 (CH_2CH_3), 15.9 (CH_2CH_3), −1.6, −2.5 ppm ($Si(CH_3)_2$); ^{31}P NMR (202 MHz, $CDCl_3$): δ = 86.7 ppm: IR (petroleum ether): $\tilde{\nu}$ = 1888 (vs), 1882 (sh), 1844 (s), 1830 cm^{-1} (m); MS (EI): *m*/*z* (%): 714 (1) [M^+], 658 (21) [M^+−2CO], 543 (1) [M^+−2CO−SiMe$_2$*t*Bu], 396 (2) [M^+−2CO−PPh$_3$], 344 (75) [M^+−Cr(CO)$_2$(PPh$_3$)], 329 (23) [M^+−Cr(CO)$_2$(PPh$_3$)−Me], 314 (22) [M^+−Cr(CO)$_2$(PPh$_3$)−2Me], 287 (13) [M^+−Cr(CO)$_2$(PPh$_3$)−*t*Bu], 262 (100) [PPh$_3^+$], 258 (26) [M^+−Cr(CO)$_2$(PPh$_3$)−*t*Bu−Et], 243 (15) [M^+−Cr(CO)$_2$(PPh$_3$)−*t*Bu−Et−Me]. HR-MS: calculated for $C_{41}H_{47}O_4SiPCr$ 714.2386, found 714.2387.

Complex **5**: Yield: 0.12 g (0.17 mmol, 31 %) of a orange-brown solid. R_f = 0.75 (dichloromethane/petroleum ether 3/2). ^{1}H NMR (300 MHz, $CDCl_3$): δ = 7.3–7.15 (m, 15H; 3C$_6$H$_5$), 5.66 (dm, $^3J_{H,H}$ = 6.6 Hz, 1H; H5/8), 5.46 (ddd, $^3J_{H,H}$ = 6.5 Hz, $^4J_{H,H}$ = 2.9 Hz, $^3J_{PH}$ = 0.9 Hz, 1H; H5/8), 4.76 ("t"dd, $^3J_{H,H}$ = 6.2 Hz, $^4J_{H,H}$ = 2.9 Hz, $^3J_{P,H}$ = 0.9 Hz, 1H; H6/7), 4.53 ("t"dd, $^3J_{H,H}$ = 6.2 Hz, $^4J_{H,H}$ = 1.9 Hz, $^3J_{P,H}$ = 0.9 Hz, 1H; H6/7), 3.72 (s, 3H; OCH_3), 2.75 (m, 2H; CH_2), 2.43 (m, 2H; CH_2), 1.08 (t, $^3J_{H,H}$ = 7.5 Hz, 3H; CH_2CH_3), 1.03 (t, $^3J_{H,H}$ = 7.5 Hz, 3H; CH_2CH_3), 1.02 (s, 9H; $C(CH_3)_3$), 0.17 (s, 3H; $SiCH_3$), 0.15 ppm (s, 3H; $SiCH_3$); ^{13}C NMR (125 MHz, $CDCl_3$): δ = 240.4 (d, $^2J_{P,C}$ = 20.6 Hz, Cr(CO)), 240.0 (d, $^2J_{P,C}$ = 19.7 Hz, Cr(CO)), 147.8, 146.6 (C1, C4), 139.4 (d, $^1J_{P,C}$ = 33.1 Hz, 3PC), 133.0 (d, $^2J_{P,C}$ = 10.6 Hz, 6PC*C*H), 130.2 (C2/3), 128.5 (3PCCH*C*H*C*H), 127.6 (d, $^3J_{P,C}$ = 8.2 Hz, 6PCCHCH*C*H*C*H), 99.7, 97.2 (C4a, C8a), 89.5, 89.3, 86.1, 80.6 (C5-C8), 61.5 (OCH_3), 26.1 ($C(CH_3)_3$), 20.4, 20.0 ($2CH_2$), 18.8 ($C(CH_3)_3$), 15.9 (CH_2CH_3), 14.7 (CH_2CH_3), −2.5, −3.2 ppm ($Si(CH_3)_2$); ^{31}P NMR (202 MHz, $CDCl_3$): δ = 90.6 ppm; IR (petroleum ether): $\tilde{\nu}$ = 1900 (vs), 1853 (s), 1844 cm^{-1} (sh); MS (EI): *m*/*z* (%): 714 (3) [M^+], 658 (55) [M^+−2CO], 396 (8) [M^+−2CO−PPh$_3$], 344 (74) [M^+−Cr(CO)$_2$(PPh$_3$)], 329 (24) [M^+−Cr(CO)$_2$(PPh$_3$)−Me], 314 (57) [M^+−Cr(CO)$_2$(PPh$_3$)−2Me], 287 (13) [M^+−Cr(CO)$_2$(PPh$_3$)−*t*Bu], 262 (100) [PPh$_3^+$], 258 (24) [M^+−Cr(CO)$_2$(PPh$_3$)−*t*Bu−Et], 243 (13) [M^+−Cr(CO)$_2$(PPh$_3$)−*t*Bu−Et−Me]. HR-MS: calculated for $C_{41}H_{47}O_4SiPCr$ 714.2386, found 714.2378.

Synthesis of dicarbonyl(triphenylphosphite)[(η^6-1,2,3,4,4a,8a)-1-*tert*-butyldimethylsilyloxy-2,3-diethyl-4-methoxynaphthalene]chromium (6) and dicarbonyl(triphenylphosphite)[(η^6-4a,5,6,7,8,8a)-1-*tert*-butyldimethylsilyloxy-2,3-diethyl-4-methoxynaphthalene]chromium (7): The reaction was carried out with tricarbonyl complex **2** (0.37 g, 0.77 mmol) and triphenylphosphite (0.20 mL, 0.77 mmol). Eluent for column chromatography: petroleum ether/dichloromethane (1/1). Overall yield: 0.38 g (0.50 mmol, 65 %) of dicarbonyl complexes **6** and **7** as a dark red solid and 0.07 g (0.15 mmol, 19 %) of unreacted tricarbonyl complex **2**. Analytical HPLC: Knauer Eurospher 100 Si, 95 % *n*-hexane, 5 % *tert*-butyl methyl ether, retention times: 3.83 min (**6**), 3.97 min (**7**).

Complex **6**: Yield: 0.29 g (0.38 mmol, 49 %) of a red-brown solid. R_f (petroleum ether/dichloromethane 1/1) = 0.40; ^{1}H NMR (500 MHz, $CDCl_3$): δ = 7.87 (m, 1H; H8/5), 7.74 (m, 1H; H5/8), 7.27–7.22, 7.09–7.02 (m, 15H; 3C$_6$H$_5$), 7.14 (m, 2H; H6, H7), 3.92 (s, 3H; OCH_3), 2.79 (dq, $^2J_{H,H}$ = 14.5 Hz, $^3J_{H,H}$ = 7.5 Hz, 1H; CH_2), 2.77 (dq, $^2J_{H,H}$ = 14.5 Hz, $^3J_{H,H}$ = 7.5 Hz, 1H; CH_2), 2.67 (dq, $^2J_{H,H}$ = 14.5 Hz, $^3J_{H,H}$ = 7.5 Hz, 1H; CH_2), 2.60 (dq, $^2J_{H,H}$ = 14.5 Hz, $^3J_{H,H}$ = 7.5 Hz, 1H; CH_2), 1.42 (t, $^3J_{H,H}$ = 7.5 Hz, 3H; CH_2CH_3), 1.32 (t, $^3J_{H,H}$ = 7.5 Hz, 3H; CH_2CH_3), 1.12 (s, 9H; $C(CH_3)_3$), 0.49 (s, 3H; $SiCH_3$), 0.41 ppm (s, 3H; $SiCH_3$); ^{13}C NMR (125 MHz, $CDCl_3$): δ = 238.6 (d, $^2J_{P,C}$ = 31.2 Hz, Cr(CO)), 236.9 (d, $^2J_{P,C}$ = 29.8 Hz, Cr(CO)), 152.4 (d, $^2J_{P,C}$ = 9.5 Hz, 3POC), 130.0 (C1/C4), 128.9 (6POCCH*C*H), 127.8 (C1/C4), 126.9, 125.9, 125.5, 124.7 (C5-C8), 123.1 (3POCCHCH*C*H), 121.0 (d, $^3J_{P,C}$ = 2.9 Hz, 6PC*C*H), 105.2, 101.3, 100.2, 98.3 (C2, C3, C4a, C8a), 63.7 (OCH_3), 26.2 ($C(CH_3)_3$), 21.0, 20.7 ($2CH_2$), 19.1 ($C(CH_3)_3$), 15.8 (CH_2CH_3), 15.6 (CH_2CH_3), −1.8, −2.9 ppm (Si-$(CH_3)_2$); ^{31}P NMR (202 MHz, $CDCl_3$): δ = 189.0; IR (petroleum ether): $\tilde{\nu}$ = 1902 (vs), 1851 (s), 1844 (sh) cm^{-1}; MS (EI): *m*/*z* (%): 762 (6) [M^+], 706 (30) [M^+−2CO], 669 (1) [M^+−OPh], 396 (3) [M^+−2CO−P(OPh)$_3$], 362 (72) [Cr(CO)$_2$P(OPh)$_3^+$], 344 (100) [M^+−Cr(CO)$_2$(P(OPh)$_3$)], 329 (43) [M^+−Cr(CO)$_2$(P(OPh)$_3$)−Me], 310 (23) [P(OPh)$_3^+$], 287 (29) [M^+−Cr(CO)$_2$(P(OPh)$_3$)−*t*Bu], 258 (41) [M^+−Cr(CO)$_2$(P(OPh)$_3$)−*t*Bu−Et], 243 (25) [M^+−Cr(CO)$_2$(P(OPh)$_3$)−*t*Bu−Et−Me], 217 (66) [P(OPh)$_2^+$], 73 (99) [SiMe$_3^+$]. HR-MS: calculated for $C_{41}H_{47}O_7SiPCr$ 762.2234, found 762.2246.

Complex **7**: Yield: 0.09 g (0.12 mmol, 16 %) of an orange-brown solid. R_f (petroleum ether/dichloromethane 1/1) = 0.40. ^{1}H NMR (500 MHz, $CDCl_3$): δ = 7.38–7.28, 7.16 (m, 15, 3C$_6$H$_5$), 5.69 (d, $^3J_{H,H}$ = 6.7 Hz, 1H; H8/5), 5.65 (d, 1H; H5/8), 4.67 (m, 1H; H6/7), 4.59 (m, 1H; H7/6), 3.88 (s, 3H; OCH_3), 2.87 (dq, $^2J_{H,H}$ = 13.6 Hz, $^3J_{H,H}$ = 7.4 Hz, 1H; CH_2), 2.83 (dq, $^2J_{H,H}$ = 14.1 Hz, $^3J_{H,H}$ = 7.4 Hz, 1H; CH_2), 2.56 (dq, $^2J_{H,H}$ = 13.6 Hz, $^3J_{H,H}$ = 7.4 Hz, 1H; CH_2), 2.49 (dq, $^2J_{H,H}$ = 14.1 Hz, $^3J_{H,H}$ = 7.4 Hz, 1H; CH_2), 1.18 (t, $^3J_{H,H}$ = 7.4 Hz, 3H; CH_2CH_3), 1.13 (s, 9H; $C(CH_3)_3$), 1.03 (t, $^3J_{H,H}$ = 7.4 Hz, 3H; CH_2CH_3), 0.22 (s, 3H; $SiCH_3$), 0.15 ppm (s, 3H; $SiCH_3$); ^{13}C NMR (125 MHz, $CDCl_3$): δ = 234.9 (d, $^2J_{P,C}$ = 32.2 Hz, Cr(CO)), 234.9 (d, $^2J_{P,C}$ = 28.0 Hz, Cr(CO)), 152.4 (d, $^2J_{P,C}$ = 6.2 Hz, 3POC), 146.8, 144.3 (C1, C4), 134.4, 130.6 (C2, C3), 129.2 (6POCCH*C*H), 123.9 (3POCCHCH*C*H), 121.8 (d, $^3J_{P,C}$ = 3.4 Hz, 6POC*C*H), 98.8, 98.6 (C4a, C8a), 89.9, 88.8, 84.0, 83.6 (C5-C8), 61.7 (OCH_3), 26.0 ($C(CH_3)_3$), 20.3, 20.0 ($2CH_2$), 18.7 ($C(CH_3)_3$), 15.8 (CH_2CH_3), 14.5 (CH_2CH_3), −2.7, −3.6 ppm ($Si(CH_3)_2$); ^{31}P NMR (202 MHz, $CDCl_3$): δ = 201.2 ppm; IR (petroleum ether): $\tilde{\nu}$ = 1930 (sh), 1922 (vs), 1884 (sh), 1875 (sh), 1869 cm^{-1} (s); MS (EI): *m*/*z* (%): 762 (6) [M^+], 706 (33) [M^+−2CO], 669 (2) [M^+−OPh], 396 (11) [M^+−2CO−P(OPh)$_3$], 362 (100) [Cr(CO)$_2$P(OPh)$_3^+$], 344 (67) [M^+−Cr(CO)$_2$(P(OPh)$_3$)], 329 (17) [M^+−Cr(CO)$_2$(P(OPh)$_3$)−Me], 310 (23) [P(OPh)$_3$], 287 (11) [M^+−Cr(CO)$_2$-(P(OPh)$_3$)−*t*Bu], 258 (20) [M^+−Cr(CO)$_2$(P(OPh)$_3$)−*t*Bu−Et], 243 (13) [M^+−Cr(CO)$_2$(P(OPh)$_3$)−*t*Bu−Et−Me], 217 (58) [P(OPh)$_2^+$]; HR-MS: calculated for $C_{41}H_{47}O_7SiPCr$ 762.2234, found 762.2213.

Synthesis of dicarbonyl(trimethylphosphine)[(η^6-1,2,3,4,4a,8a)-1-*tert*-butyldimethylsilyloxy-2,3-diethyl-4-methoxynaphthalene]chromium (8) and dicarbonyl(trimethylphosphine)[(η^6-4a,5,6,7,8,8a)-1-*tert*-butyldimethylsilyloxy-2,3-diethyl-4-methoxynaphthalene]chromium (9): The reaction was carried out with tricarbonyl complex **2** (0.39 g, 0.81 mmol) and trimethylphosphine solution in toluene: (8.0 mL, 1 M, 8.0 mmol). Eluent for column chromatography: petroleum ether/dichloromethane (4/3). Overall

yield: 0.26 g (0.49 mmol, 61%) of a black solid. Analytical HPLC: Knauer Eurospher 100 CN, 95% *n*-hexane, 5% *tert*-butyl methyl ether, retention times: 4.62 min (**8**), 5.83 min (**9**).

Complex **8**: Yield: 0.22 g (0.42 mmol, 52%) of a brown solid. R_f (petroleum ether/dichloromethane 4/3)= 0.15; ^{1}H NMR (500 MHz, CD_2Cl_2): δ=7.80 (dm, $^3J_{H,H}$=8.6 Hz, 1H; H5/8), 7.72 (dm, $^3J_{H,H}$=8.2 Hz, 1H; H5/8), 7.27–7.19 (m, 2H; H6/7), 3.85 (s, 3H; $COCH_3$), 2.83 (dq, $^2J_{H,H}$= 14.3 Hz, $^3J_{H,H}$=7.5 Hz, 1H; CH_2), 2.69 (dq, $^2J_{H,H}$=14.3 Hz, $^3J_{H,H}$=7.5 Hz, 1H; CH_2), 2.66 (dq, $^2J_{H,H}$=14.4 Hz, $^3J_{H,H}$=7.5 Hz, 1H; CH_2), 2.61 (dq, $^2J_{H,H}$=14.4 Hz, $^3J_{H,H}$=7.5 Hz, 1H; CH_2), 1.33 (t, $^3J_{H,H}$=7.5 Hz, 3H; CH_2CH_3), 1.31 (t, $^3J_{H,H}$=7.5 Hz, 3H; CH_2CH_3), 1.07 (s, 9H; $C(CH_3)_3$), 1.07 (d, $^3J_{PH}$=7.9 Hz, $P(CH_3)_3$), 0.41 (s, 3H; $SiCH_3$), 0.35 ppm (s, 3H; $SiCH_3$); ^{13}C NMR (125 MHz, CD_2Cl_2): δ=240.5 (d, $^2J_{P,C}$=21.1 Hz, Cr(CO)), 239.0 (d, $^2J_{P,C}$=20.2 Hz, Cr(CO)), 128.2 (C1/4), 125.5, 125.4 (2 ArCH), 125.0 (C1/4), 124.9, 124.4 (2 ArCH), 101.8, 99.8, 99.8, 98.9 (C2, C3, C4a, C8a), 63.2 (OCH_3), 26.1 ($C(CH_3)_3$), 21.5, 20.9 ($2CH_2$), 19.0 (d, $^1J_{P,C}$=22.1 Hz, $P(CH_3)_3$), 18.9 ($C(CH_3)_3$), 16.2 (CH_2CH_3), 15.9 (CH_2CH_3), −2.1, −3.1 ppm ($Si(CH_3)_2$); ^{31}P NMR (202 MHz, CD_2Cl_2): δ=35.0 ppm; IR (petroleum ether): $\tilde{\nu}$=1888 (w), 1878 (vs), 1838 (sh), 1826 cm^{-1} (s); MS (EI): *m*/*z* (%): 528 (1), 472 (10) [M^+−2CO], 396 (5) [M^+ −2CO−PMe_3], 344 (77) [M^+−$Cr(CO)_2(PMe_3)$], 329 (42) [M^+−$Cr(CO)_2$-(PMe_3)−Me], 287 (25) [M^+−$Cr(CO)_2(PMe_3)$−*t*Bu], 258 (37) [M^+ −$Cr(CO)_2(PMe_3)$−*t*Bu−Et], 243 (21) [M^+−$Cr(CO)_2(PMe_3)$ −*t*Bu−Et−Me], 73 (100) [$SiMe_3^+$]; HR-MS: calculated for $C_{26}H_{41}O_4$-SiPCr 528.1917, found 528.1909.

Complex **9**: (0.04 g, 0.08 mmol, 10%) of a red solid. R_f (petroleum ether/dichloromethane 4/3)=0.15; ^{1}H NMR (500 MHz, CD_2Cl_2): δ=5.85 (ddd, $^3J_{H,H}$=6.5 Hz, $^4J_{H,H}$=3.2 Hz, $^3J_{PH}$=1.0 Hz, 1H; H5/8), 5.80 (ddd, $^3J_{H,H}$= 6.6 Hz, $^4J_{H,H}$=4.0 Hz, $^3J_{PH}$=1.0 Hz, 1H; H5/8), 5.12 ("t"d, $^3J_{H,H}$=6.2 Hz, $^3J_{PH}$=1.0 Hz, 1H; H6/7), 5.00 ("t"d, $^3J_{H,H}$=6.2 Hz, $^3J_{PH}$=1.0 Hz, 1H; H6/7), 3.93 (s, 3H; OCH_3), 2.86 (dq, $^2J_{H,H}$=13.6 Hz, $^3J_{H,H}$=7.5 Hz, 1H; CH_2), 2.82 (dq, $^2J_{H,H}$=13.7 Hz, $^3J_{H,H}$=7.5 Hz, 1H; CH_2), 2.53 (dq, $^2J_{H,H}$= 13.6 Hz, $^3J_{H,H}$=7.5 Hz, 1H; CH_2), 2.49 (dq, $^2J_{H,H}$=13.6 Hz, $^3J_{H,H}$=7.5 Hz, 1H; CH_2), 1.16 (t, $^3J_{H,H}$=7.5 Hz, 3H; CH_2CH_3), 1.10 (s, 9H; $C(CH_3)_3$), 1.07 (d, $^2J_{P,H}$=8.0 Hz, 9H; $P(CH_3)_3$), 1.01 (t, $^3J_{H,H}$=7.5 Hz, 3H; CH_2CH_3), 0.25 (s, 3H; $SiCH_3$), 0.19 ppm (s, 3H; $SiCH_3$); ^{31}P NMR (202 MHz, CD_2Cl_2): δ=33.4 ppm. IR (petroleum ether): $\tilde{\nu}$=1898 (vs), 1892 (s), 1844 (s), 1836 cm^{-1} (m); MS (EI): *m*/*z* (%): 528 (4), 472 (23) [M^+−2CO], 396 (10) [M^+−2CO−PMe_3], 344 (100) [M^+−$Cr(CO)_2$-(PMe_3)], 329 (45) [M^+−$Cr(CO)_2(PMe_3)$ −Me], 287 (25) [M^+−$Cr(CO)_2$-(PMe_3)−*t*Bu], 258 (37) [M^+−$Cr(CO)_2(PMe_3)$−*t*Bu−Et], 243 (22) [M^+ −$Cr(CO)_2(PMe_3)$ −*t*Bu−Et−Me], 73 (60) [$SiMe_3^+$]. HR-MS: calculated for $C_{26}H_{41}O_4SiPCr$ 528.1917, found 528.1925.

Synthesis of dicarbonyl(trimethylphosphite)[(η^6-1,2,3,4,4a,8a)-1-*tert*-butyldimethylsilyloxy-2,3-diethyl-4-methoxynaphthalene]chromium (10) and dicarbonyl(trimethylphosphite)[(η^6-4a,5,6,7,8,8a)-1-*tert*-butyldimethylsilyloxy-2,3-diethyl-4-methoxynaphthalene]chromium (11): The reaction was carried out with tricarbonyl complex **2** (0.36 g, 0.75 mmol) and trimethylphosphite (1.0 mL, 8.5 mmol). Eluent for column chromatography: dichloromethane. Overall yield: 0.26 g (0.47 mmol, 60%) of the dicarbonyl complexes **10** and **11** as a dark red solid and unreacted starting material **2** (0.13 g, 0.27 mmol; 36%). Analytical HPLC: Knauer Eurospher 100 Si, 95% *n*-hexane, 5% *tert*-butyl methyl ether, retention times: 6.15 min (**10**), 8.15 min (**11**). Complex **10**: Yield: 0.22 g (0.38 mmol, 51%) of a dark red solid. R_f (dichloromethane)=0.46; ^{1}H NMR (300 MHz, $CDCl_3$): δ=7.85 (d, $^3J_{H,H}$=8.5 Hz, 1H; H5/8), 7.72 (d, $^3J_{H,H}$=8.1 Hz, 1H; H5/8), 7.35–7.20 (m, 2H; H6, H7), 3.86 (s, 3H; $COCH_3$), 2.99 (dq, $^2J_{H,H}$= 14.5 Hz, $^3J_{H,H}$=7.5 Hz, 1H; CH_2), 2.72 (m, 3H; CH_2), 1.36 (t, $^3J_{H,H}$= 7.5 Hz, 3H; CH_2CH_3), 1.33 (t, $^3J_{H,H}$=7.5 Hz, 3H; CH_2CH_3), 1.09 (s, 9H; $C(CH_3)_3$), 0.40 (s, 3H; $SiCH_3$), 0.32 ppm (s, 3H; $SiCH_3$); ^{13}C NMR (125 MHz, $CDCl_3$): δ=239.1 (d, $^2J_{P,C}$=33.1 Hz, Cr(CO)), 237.7 (d, $^2J_{P,C}$= 31.7 Hz, Cr(CO)), 128.0, 128.0 (C1, C4), 126.6, 126.0, 124.9, 124.6 (C5-C8), 104.5, 100.0, 99.9, 97.0 (C2, C3, C4a, C8a), 63.4 (OCH_3), 26.2 (C-(CH_3)$_3$), 21.6, 20.8 ($2CH_2$), 19.1 ($C(CH_3)_3$), 16.2 (CH_2CH_3), 15.7 (CH_2CH_3), −1.8, −2.7 ppm ($Si(CH_3)_2$); ^{31}P NMR (202 MHz, $CDCl_3$): δ= 213.3 ppm; IR (petroleum ether): $\tilde{\nu}$=1898 (s), 1886 (vs), 1846 (m), 1836 cm^{-1} (s); MS (EI): *m*/*z* (%): 576 (10) [M^+], 545 (5) [M^+−OMe], 520 (61) [M^+−2CO], 396 (74) [M^+−2CO−$P(OMe)_3$], 344 (74) [M^+ −$Cr(CO)_2(P(OMe)_3)$], 329 (35) [M^+−$Cr(CO)_2(P(OMe)_3)$−Me], 287 (25) [M^+−$Cr(CO)_2(P(OMe)_3)$−*t*Bu], 258 (37) [M^+−$Cr(CO)_2$-($P(OMe)_3$)−*t*Bu−Et], 243 (29) [M^+−$Cr(CO)_2(P(OMe)_3)$−*t*Bu−Et−Me], 176 (22) [$Cr(P(OMe)_3^+$], 73 (100) [$SiMe_3^+$]; HR-MS: calculated for $C_{26}H_{41}O_7SiPCr$ 576.1764, found 576.1757.

Complex **11**: R_f (dichloromethane)=0.46; ^{1}H NMR (500 MHz, $CDCl_3$): δ=6.04 (dm, $^3J_{H,H}$=6.5 Hz, 1H; H5/8), 6.00 (dm, $^3J_{H,H}$=6.5 Hz, 1H; H5/8), 5.23 ("t", $^3J_{H,H}$=6.2 Hz, 1H; H6/7), 5.16 ("t", $^3J_{H,H}$=6.2 Hz, 1H; H6/7), 3.92 (s, 3H; OCH_3), 3.29 (d, ", $^3J_{PH}$=11.4 Hz, 9H; $P(OCH_3)_3$), 2.87 (dq, $^2J_{H,H}$=13.3 Hz, $^3J_{H,H}$=7.4 Hz, 1H; CH_2), 2.81 (dq, $^2J_{H,H}$=13.5 Hz, $^3J_{H,H}$=7.4 Hz, 1H; CH_2), 2.53 (dq, $^2J_{H,H}$=13.3 Hz, $^3J_{H,H}$=7.4 Hz, 1H; CH_2), 2.48 (dq, $^2J_{H,H}$=13.5 Hz, $^3J_{H,H}$=7.4 Hz, 1H; CH_2), 1.17 (t, $^3J_{H,H}$= 7.4 Hz, 3H; CH_2CH_3), 1.08 (s, 9H; $C(CH_3)_3$), 1.01 (t, $^3J_{H,H}$=7.4 Hz, 3H; CH_2CH_3), 0.22 ppm (s, 6H; $Si(CH_3)_2$); ^{13}C NMR (125 MHz, $CDCl_3$): δ= 237.4 (d, $^2J_{P,C}$=32.2 Hz, Cr(CO)), 237.0 (d, $^2J_{P,C}$=31.7 Hz, Cr(CO)), 147.2, 144.6 (C1, C4), 133.9, 130.0 (C2, C3), 100.3, 99.4 (C4a, C8a), 88.5, 88.2, 82.2, 81.8 (C5-C8), 61.8 (OCH_3), 26.0 ($C(CH_3)_3$), 20.4, 20.0 ($2CH_2$), 18.7 ($C(CH_3)_3$), 15.7 (CH_2CH_3), 14.3 (CH_2CH_3), −2.5, −3.3 ppm ($Si(CH_3)_2$); ^{31}P NMR (202 MHz, $CDCl_3$): δ=214.7 ppm; IR (petroleum ether): $\tilde{\nu}$=1909 (vs), 1900 (sh), 1853 cm^{-1} (s); MS (EI): *m*/*z* (%): 576 (1) [M^+], 545 (1) [M^+−OMe], 520 (7) [M^+−2CO], 396 (8) [M^+−2CO−P-($OMe)_3$], 344 (42) [M^+−$Cr(CO)_2(P(OMe)_3)$], 329 (23) [M^+−$Cr(CO)_2$-($P(OMe)_3$)−Me], 287 (17) [M^+−$Cr(CO)_2(P(OMe)_3)$−*t*Bu], 258 (29) [M^+ −$Cr(CO)_2(P(OMe)_3)$ −*t*Bu−Et], 243 (22) [M^+−$Cr(CO)_2$-($P(OMe)_3$)−*t*Bu−Et−Me], 73 (100) [$SiMe_3^+$]; HR-MS: calculated for $C_{26}H_{41}O_7SiPCr$ 576.1764, found 576.1767.

Procedure for the kinetic analyses: For the kinetic studies of the haptotropic metal shift, the thermodynamically less favourable isomers were dissolved in distilled NMR-grade hexafluorobenzene, which was carefully deoxygenated prior to each use. The solution was filtered into a dry, argon-flushed NMR tube which was sealed after inserting the external standard ([D_8]dioxane). ^{1}H NMR spectra were recorded in appropriate intervals (5 to 20 min) at the specified temperature. The relative concentration of the two isomers was determined by the integration of the signals for the hydrogen atoms of the dimethyl(silyl) fragment.

Acknowledgements

Financial support from the Deutsche Forschungsgemeinschaft (SFB 624) is gratefully acknowledged. H.C.J. thanks the Fonds der Chemischen Industrie for providing a doctoral grant.

[1] a) B. Deubzer, H. P. Fritz, C. G. Kreiter, K. Öfele, *J. Organomet. Chem.* **1967**, *7*, 289–299; b) J. Müller, P. Göser, M. Elian, *Angew. Chem.* **1969**, *81*, 331–332; *Angew. Chem. Int. Ed. Engl.* **1969**, *8*, 374–375; c) K. M. Nicholas, R. C. Kerber, E. I. Stiefel, *Inorg. Chem.* **1971**, *10*, 1519–1521; d) T. A. Albright, P. Hofmann, R. Hoffmann, C. P. Lillya, P. A. Dobosh, *J. Am. Chem. Soc.* **1983**, *105*, 3396–3411; e) B. E. Mann, *Chem. Soc. Rev.* **1986**, *15*, 167–187; f) E. P. Kündig, V. Desorby, C. Grivet, B. Rudolph, S. Spichiger, *Organometallics* **1987**, *6*, 1173–1180; g) P. Berno, A. Ceccon, A. Gambaro, A. Venzo, P. Ganis, G. Valle, *J. Chem. Soc. Perkin Trans. 2* **1987**, 935–941; h) Y. F. Oprunenko, S. G. Malugina, Y. A. Ustynyuk, N. A. Ustynyuk, D. N. Kravtsov, *J. Organomet. Chem.* **1988**, *338*, 357–368; i) Y. F. Oprunenko, *Russ. Chem. Rev.* **2000**, *69*, 683–704, and references therein.

[2] C. White, J. Thompson, P. M. Maitlis, *J. Chem. Soc. Dalton Trans.* **1977**, 1654–1661.

[3] a) Y. F. Oprunenko, N. G. Akhmedov, D. N. Laikov, A. G. Malyugina, V. I. Mstislavsky, V. A. Roznyatovsky, Y. A. Ustynyuk, N. A. Ustynyuk, *J. Organomet. Chem.* **1999**, *583*, 136–145; b) K. H. Dötz, N. Szesni, M. Nieger, K. Nättinen, *J. Organomet. Chem.* **2003**, *671*, 58–74; c) K. H. Dötz, H. C. Jahr, *Chem. Rec.* **2004**, *4*, 61–71.

[4] a) H. C. Jahr, M. Nieger, K. H. Dötz, *J. Organomet. Chem.* **2002**, *641*, 185–194; b) H. C. Jahr, M. Nieger, K. H. Dötz, unpublished results; c) J. Stendel, Jr., K. H. Dötz, unpublished results.
[5] a) Y. Oprunenko, S. Malyugina, P. Nesterenko, D. Mityuk, O. Malyshev, *J. Organomet. Chem.* **2000**, *597*, 42–47; b) H. C. Jahr, M. Nieger, K. H. Dötz, *Chem. Commun.* **2003**, 2866–2867.
[6] a) K. H. Dötz, P. Tomuschat, *Chem. Soc. Rev.* **1999**, *28*, 187–198; b) K. H. Dötz, J. Stendel, Jr. , in *Modern Arene Chemistry* (Ed.: D. Astruc), Wiley-VCH, Weinheim, **2002**, p. 250–296; c) K. H. Dötz, B. Wenzel, H. C. Jahr in *Templates in Chemistry I* (Eds.: C. A. Schalley, F. Vögtle, K. H. Dötz), Springer, Berlin, **2004**.
[7] E. P. Kündig, V. Desorby, D. P. Simmons, E. Wenger, *J. Am. Chem. Soc.* **1989**, *111*, 1804–1814.
[8] G. Jaouen, *Tetrahedron Lett.* **1973**, *14*, 5159–5162.
[9] D. Paetsch, K. H. Dötz, *Tetrahedron Lett.* **1999**, *40*, 487–488.
[10] L. F. Veiros, *Organometallics* **2000**, *19*, 3127–3136.
[11] C. A. Tolman, *Chem. Rev.* **1977**, *77*, 313–348.
[12] T. Bartik, T. Himmler, H.-G. Schulte, K. Seevogel, *J. Organomet. Chem.* **1984**, *272*, 29–41.
[13] a) M. N. Golovin, M. M. Rahman, J. E. Belmonte, W. P. Giering, *Organometallics* **1985**, *4*, 1981–1991; b) M. M. Rahman, H. Y. Liu, A. Prock, W. P. Giering, *Organometallics* **1987**, *6*, 650–658.
[14] a) J. M. Hanckel, K.-W. Lee, P. Rushman, T. L. Brown, *Inorg. Chem.* **1986**, *25*, 1852–1856; b) L. Stahl, R. D. Ernst, *J. Am. Chem. Soc.* **1987**, *109*, 5673–5680; c) L. Stahl, W. Trakarnpruk, J. W. Freeman, A. M. Arif, R. D. Ernst, *Inorg. Chem.* **1995**, *34*, 1810–1814; d) J. M. Smith, N. J. Coville, L. M. Cook, J. C. A. Boeyens, *Organometallics* **2000**, *19*, 5273–5280; e) J. M. Smith, N. J. Coville, *Organometallics* **2001**, *20*, 1210–1215; f) K. A. Bunten, L. Chen, A. L. Fernandez, A. J. Poë, *Coord. Chem. Rev.* **2002**, *233–234*, 41–51.

Received: July 2, 2004
Revised: February 24, 2005
Please note: Minor changes have been made to this manuscript since its publication in *Chemistry—A European Journal* Early View. The Editor.
Published online: July 8, 2005